The Journal of Neuroscience, June 15, 1998, *18*(12):4461–4472

Identification of Four Classes of Brain Nicotinic Receptors Using β2 Mutant Mice

Michele Zoli,[1,2] Clément Léna,[1] Marina R. Picciotto,[1,3] and Jean-Pierre Changeux[1]

[1]*Centre National de la Recherche Scientifique Unité de Recherche Associée D1284, Neurobiologie Moléculaire, Institut Pasteur, 75724 Paris Cédex 15, France,* [2]*Section of Physiology, Department of Biomedical Sciences, University of Modena, Modena, Italy, and* [3]*Department of Psychiatry, Yale University School of Medicine, New Haven, Connecticut 06508*

Although the expression patterns of the neuronal nicotinic acetylcholine receptor (nAChR) subunits thus far described are known, the subunit composition of functional receptors in different brain areas is an ongoing question. Mice lacking the β2 subunit of the nAChR were used for receptor autoradiography studies and patch-clamp recording in thin brain slices. Four distinct types of nAChRs were identified, expanding on an existing classification [Alkondon M, Albuquerque EX (1993) Diversity of nicotinic acetylcholine receptors in rat hippocampal neurons. I. Pharmacological and functional evidence for distinct structural subtypes. J Pharmacol Exp Ther 265:1455–1473.], and tentatively identifying the subunit composition of nAChRs in different brain regions. Type 1 nAChRs bind α-bungarotoxin, are not altered in β2 −/− mice, and contain the α7 subunit. Type 2 nAChRs contain the β2 subunit because they are absent in β2 −/− mice, bind all nicotinic agonists used with high affinity (excluding α-bungarotoxin), have an order of potency for nicotine ≫ cytisine in electrophysiological experiments, and are likely to be composed of α4β2 in most brain regions, with other α subunits contributing in specific areas. Type 3 nAChRs bind epibatidine with high affinity in equilibrium binding experiments and show that cytisine is as effective as nicotine in electrophysiological experiments; their distribution and persistence in β2 −/− mice strongly suggest a subunit composition of α3β4. Type 4 nAChRs bind cytisine and epibatidine with high affinity in equilibrium binding experiments and persist in β2 −/− mice; cytisine = nicotine in electrophysiological experiments. Type 4 nAChRs also exhibit faster desensitization than type 3 nAChRs at high doses of nicotine. Knock-out animals lacking individual α subunits should allow a further dissection of nAChR subclasses.

Key words: nicotinic receptor; receptor classification; homologous recombination; patch clamp; receptor autoradiography; mouse; CNS

Neuronal nicotinic acetylcholine receptors (nAChRs) comprise a family of pentameric oligomers made up of combinations of 10 different subunits (for review, see Le Novère and Changeux, 1995). The α subunits (α2–α8) contain two cysteines that contribute to acetylcholine (ACh) binding, whereas the non-α or β subunits (β2–β4) lack these residues but contribute to the complementary component of the binding site and affect the pharmacological properties of the receptor (Luetje and Patrick, 1991). On the basis of phylogenetic and pharmacological properties (Le Novère and Changeux, 1995), the α7 and α8 subunits comprise an α-bungarotoxin-sensitive subfamily of nAChRs that can form functional homo-oligomers in reconstituted systems (Couturier et al., 1990). The α2–α6 and β2–β4 subunits comprise a second subfamily that can combine to form a number of functionally different hetero-oligomers (Sargent, 1993; Role and Berg, 1996). α9 is in a third family and is expressed in non-neuronal cells in the cochlea (Elgoyhen et al., 1994).

α-Bungarotoxin binding is considered to represent the distribution of α7 subunit-containing nAChRs (Orr-Utreger et al., 1997). However, most nicotinic ligands show similar patterns of high-affinity labeling (Clarke et al., 1985; Happe et al., 1994; Aubert et al., 1996) that resembles the distribution of α4/β2 in the brain (Wada et al., 1989; Hill et al., 1993). More recently, epibatidine has been shown to bind with very high affinity to nAChRs (Houghtling et al., 1995), with a distribution comparable to that of ^{3}H-nicotine (Perry and Kellar, 1995), and to exert a number of classical effects of central nicotinic agonists (Badio and Daly, 1994; Sullivan et al., 1994; Gerzanich et al., 1995).

In the mammalian brain, patch-clamp recording demonstrates at least two different nAChRs in the habenulo-interpeduncular system, putatively α3/β4 and α2/β4, based on subunit distribution and on comparison with specific isotypes reconstituted in *Xenopus* oocytes (Mulle et al., 1991; Connolly et al., 1995). In a series of papers in which electrophysiological recordings were performed along with *in situ* hybridization, several nAChR populations have been characterized in the hippocampal formation of the rat containing α7, α4β2, and α3β4 (Alkondon and Albuquerque, 1993, 1995; Alkondon et al., 1994).

Mice lacking the gene for the β2 nAChR subunit have no detectable high-affinity ^{3}H-nicotine binding in the brain (Picciotto et al., 1995). Here we show the persistence of high-affinity binding for a number of other nicotinic ligands in mutant animals.

Received Nov. 13, 1997; revised March 30, 1998; accepted March 30, 1998.

This work was supported by the Collège de France, the Centre National pour la Recherche Scientifique, the Association Francaise contre la Myopathie, the Council for Tobacco Research, Biomed and Biotech contracts from the Commission of the European Communities, and a grant from the Human Frontier Program. C.L. was supported by a Roux grant from the Institut Pasteur; M.R.P. was supported by grants from the Donaghue Foundation, National Alliance for Research on Schizophrenia and Depression, and Grant DA10455 from National Institutes of Health. We thank Dr. Nicolas Le Novère for his careful reading of this manuscript and for useful discussions.

Correspondence should be addressed to Dr. Jean-Pierre Changeux, Neurobiologie Moléculaire, Institut Pasteur, 28 Rue du Dr. Roux, 75724 Paris Cédex 15, France.

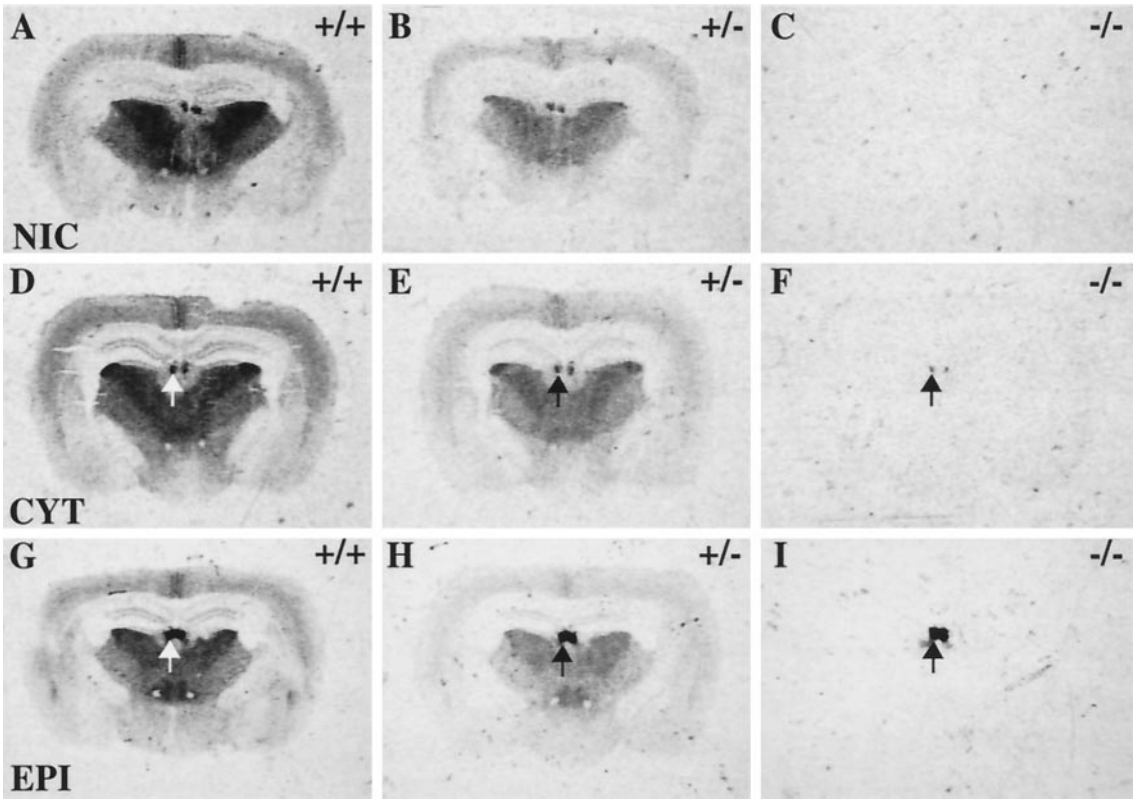

Figure 1. Film autoradiograms of ^{3}H-nicotine, ^{3}H-cytisine, and ^{3}H-epibatidine binding at bregma level −1.5 mm of β2 +/+, +/−, and −/− mice. The *arrow* indicates the medial habenula. Both ^{3}H-cytisine and ^{3}H-epibatidine binding persist in the medial habenula of β2 −/− mice. However, ^{3}H-epibatidine is distributed homogeneously in the medial habenula, whereas ^{3}H-cytisine binding is markedly more concentrated in the lateral than in the medial portion of this nucleus. *CYT*, Cytisine; *EPI*, epibatidine; *NIC*, nicotine.

The distribution of other β subunits is not widespread in wild-type rodents (Dineley-Miller et al., 1992; Le Novère et al., 1996), and there is no up- or downregulation of expression of other nicotinic subunits in mutant animals (Picciotto et al., 1995); therefore, nAChR binding is restricted to a limited number of regions. Regional analysis of binding was followed by an exploratory survey of residual nAChRs, using patch-clamp recording in brain slices. We interpret the differences of binding and activation properties of the ligands in the different brain structures as a consequence of differences in the subunit composition of the nAChRs, and we expand the existing classification of nAChR subtypes (Alkondon and Albuquerque, 1993).

MATERIALS AND METHODS

Animals

Mice were generated by mating parents heterozygous for a mutation in the β2 subunit of the neuronal nAChR (Picciotto et al., 1995). The genotype of the offspring was determined by PCR, using oligonucleotides identifying the mutant and wild-type copies of the β2 gene. In each experiment, mice homozygous for the mutation in the β2 gene were paired with heterozygous and wild-type β2 mice of the same sex and from the same litter. All experiments were performed on brains from mice between 4 and 7 months of age.

Materials

^{3}H-Nicotine, ^{3}H-methylcarbamylcholine, ^{3}H-cytisine, ^{3}H-pirenzepine, and ^{3}H-AF-DX384 were obtained from New England Nuclear (Boston, MA). ^{3}H-Epibatidine and ^{125}I-α-bungarotoxin were purchased from Amersham (Arlington Heights, IL). ^{3}H-Acetylcholine iodide was obtained from Isotopchim. Unlabeled nicotine, cytisine, atropine, and dimethylphenylpiperazinium (DMPP) were purchased from Sigma (St. Louis, MO), whereas epibatidine, dihydro-β-erythroidine (DHβE), mecamylamine (MCA), and methyllycaconitine (MLA) were obtained from Research Biochemicals (Natick, MA).

Receptor autoradiography

Mice were decapitated, and brains were dissected out and frozen in crushed dry ice. Sections (14 μm) were cut at the cryostat (Reichert-Jung), mounted on gelatinized slides, and stored for not more than 2 d at −80°C until use. In the analysis of nicotinic ligand binding, sections were taken at 15 coronal levels [bregma levels: 1.2, 1.0, 0.4, −0.2, −0.5, −1.5, −2.0, −2.9, −3.4, −3.9, −4.8, −5.3, −5.8, 7.0, and −7.5 mm, according to Franklin and Paxinos (1997)]. In the analysis of ^{125}I-α-bungarotoxin binding, sections were taken at 10 coronal levels: 1.0, 0.4, −0.5, −1.5, −2.0, −3.4, −4.8, −5.3, −5.8, and −7.5 mm. In the analysis of muscarinic ligands, sections were taken at five coronal levels: 0.4, −0.5, −1.5, −3.4, and −5.3 mm.

On the day of the experiment the slides were thawed and processed according to established protocols (see below for details) (Wamsley et al., 1984; Clarke et al., 1985; Cortes et al., 1986; Regenold et al., 1987; Happe et al., 1994; Perry and Kellar, 1995; Aubert et al., 1996). The concentration of radioactive ligands used in the experiments was close to the K_D as reported in previous papers, using receptor autoradiography or homogenate binding. In each experiment, sections from a β2 +/+, +/−, and −/− mouse were processed in parallel. For each ligand at least five brains of each genotype were used. Slides were exposed to ^{3}H-Hyperfilm (Amersham) for the length of time indicated and developed in Eastman Kodak (Rochester, NY) D19 film developer (4 min at 22°C).

Quantitative receptor autoradiography was performed by means of computer-assisted microdensitometry (VIDAS image analyzer, Kontron, Munich, Germany) and by using appropriate standards (Benfenati et al., 1986). Statistical analysis was performed according to the Mann–Whitney *U* test.

^{3}H-Nicotine (85 Ci/mmol) was used at a concentration of 5 nM. The incubation was performed at room temperature for 30 min in 50 mM Tris-HCl, pH 7.4. It was followed by four rinses of 30 sec in the same buffer, followed by a brief rinse in distilled water, all performed at 4°C.

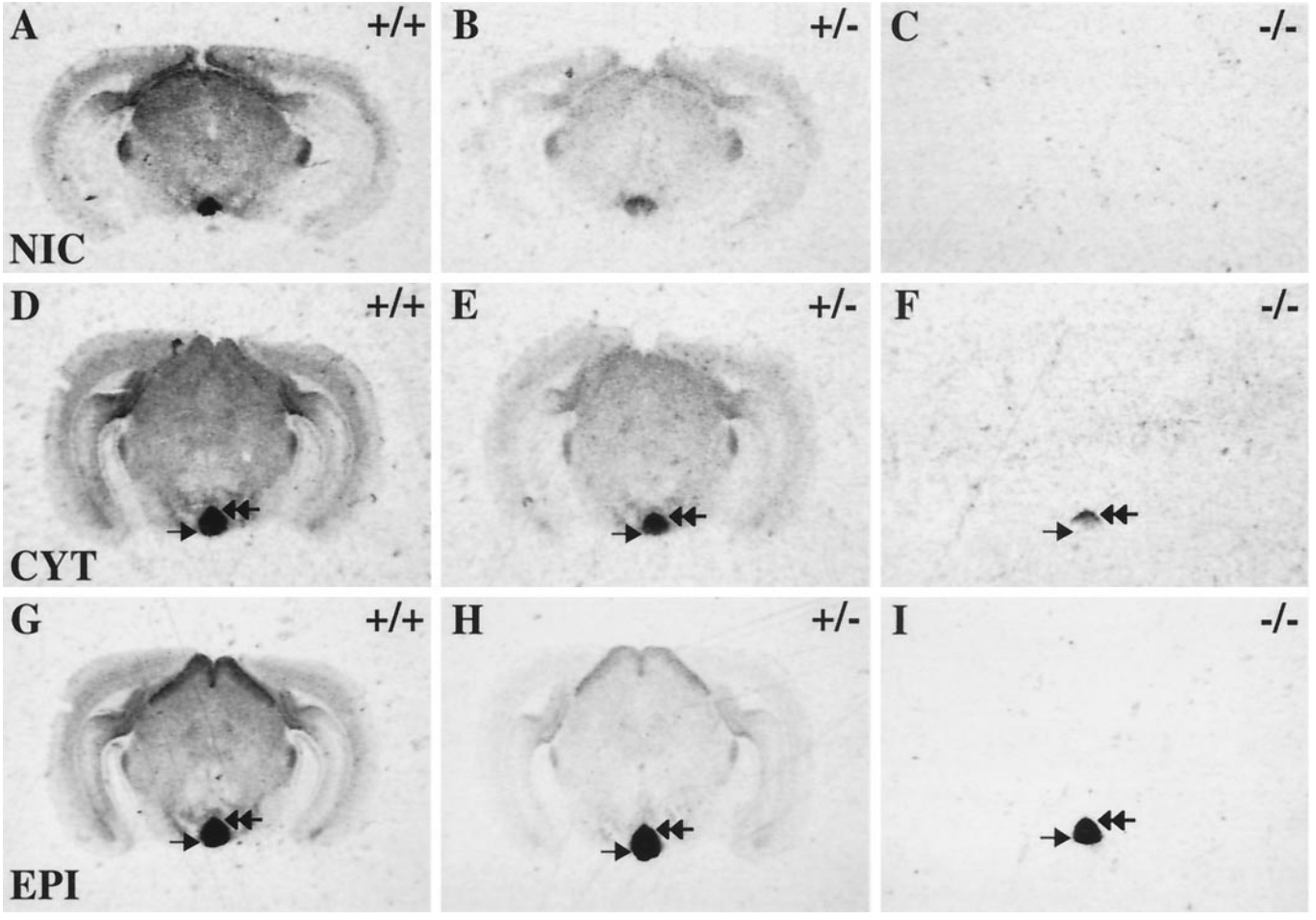

Figure 2. Film autoradiograms of ^{3}H-nicotine, ^{3}H-cytisine, and ^{3}H-epibatidine binding at bregma level −3.4 mm of β2 +/+, +/−, and −/− mice. The *arrow* and *double arrow* indicate the ventral and dorsal interpeduncular nucleus, respectively. Both ^{3}H-cytisine and ^{3}H-epibatidine binding persist in the interpeduncular nucleus of β2 −/− mice. However, ^{3}H-epibatidine is distributed homogeneously in the interpeduncular nucleus, whereas ^{3}H-cytisine binding is markedly more concentrated in the dorsal than in the ventral portion of this nucleus. For abbreviations, see the legend to Figure 1.

Nonspecific binding was defined as the binding in the presence of cold nicotine (10 μM). The film exposure time was 3 months.

^{3}H-Cytisine (30 Ci/mmol) was used at a concentration of 5 nM. The incubation was performed at 4°C for 60 min in 50 mM Tris-HCl, pH 7.4, containing (in mM) 120 NaCl, 5 KCl, 2.5 $CaCl_2$, and 1 $MgCl_2$. It was followed by three rinses for 2.5 min in 50 mM Tris-HCl, pH 7.4, followed by a brief rinse in distilled water, all performed at 4°C. Nonspecific binding was defined as the binding in the presence of cold nicotine (10 μM). The film exposure time was 3 months.

^{3}H-Methylcarbamylcholine (84 Ci/mmol) was used at a concentration of 5 nM. The incubation was performed at room temperature for 30 min in 50 mM Tris-HCl, pH 7.4. It was followed by two rinses of 30 sec in the same buffer, followed by a brief rinse in distilled water, all performed at 4°C. Nonspecific binding was defined as the binding in the presence of cold nicotine (10 μM). The film exposure time was 3 months.

^{3}H-Acetylcholine (84 Ci/mmol) was used at a concentration of 10 nM. Two preincubations were performed at room temperature for 15 and 10 min in 50 mM Tris-HCl, pH 7.4, containing (in mM) 120 NaCl, 5 KCl, 2 $CaCl_2$, and 1 $MgCl_2$ plus 1.5 μM atropine. The incubation was performed in the same buffer for 60 min at 4°C. It was followed by two rinses of 2 min in 50 mM Tris-HCl, pH 7.4, followed by a brief rinse in distilled water, all performed at 4°C. Nonspecific binding was defined as the binding in the presence of cold nicotine (10 μM). The film exposure time was 3 months.

^{3}H-Epibatidine (53 Ci/mmol) was used at a concentration of 200 pM. The incubation was performed at room temperature for 30 min in 50 mM Tris-HCl, pH 7.4. It was followed by two rinses of 5 min in the same buffer, followed by a brief rinse in distilled water, all performed at 4°C. Nonspecific binding was defined as the binding in the presence of cold nicotine (10 μM). The film exposure time was 2–4 months.

^{125}I-α-Bungarotoxin (2000 Ci/mmol) was used at a concentration of 1.5 nM. The preincubation and incubation were performed at room temperature for 30 and 120 min, respectively, in 50 mM Tris-HCl, pH 7.4, containing 0.1% bovine serum albumin. They were followed by six rinses of 30 min in 50 mM Tris-HCl, pH 7.4, and a brief rinse in distilled water, all performed at 4°C. Nonspecific binding was defined as the binding in the presence of cold nicotine (1 mM). The film exposure time was 1–2 d.

^{3}H-Pirenzepine and ^{3}H-AF-DX384 (78 and 120 Ci/mmol, respectively) were used at a concentration of 10 nM. The preincubation and incubation were performed at room temperature for 15 and 60 min, respectively, containing (in mM) 120 NaCl, 1.2 $MgSO_4$, 1.2 KH_2PO_4, 25 $NaHCO_3$, 2.5 $CaCl_2$, 4.7 KCl, and 5.6 glucose, pH 7.4. They were followed by three rinses for 4 min in 50 mM Tris-HCl, pH 7.4, and a brief rinse in distilled water, all performed at 4°C. Nonspecific binding was defined as the binding in the presence of cold atropine (1.5 μM). The film exposure time was 1 month.

In situ *hybridization*

After analysis for mRNA secondary structure via GCG Sequence Analysis Software 7.1, three oligodeoxynucleotide sequences were chosen in unique regions of the rat α3, α5, and β4 mRNAs and synthesized with a Cyclone (Biosearch) DNA synthesizer. The probe characteristics and specificity controls are reported in Zoli et al. (1995) and Le Novère et al. (1996). Specificity control included the demonstration that (1) two or more probes for each mRNA give identical labeling pattern, (2) the labeling disappears when labeled probes are incubated with an excess of cold probe, and (3) probes with the same base composition but different sequence do not give the specific labeling pattern. The oligonucleotide probes were labeled at the 3′ end, using ^{35}S-dATP (Amersham) and terminal deoxynucleotidyl transferase (Boehringer Mannheim, Indianap

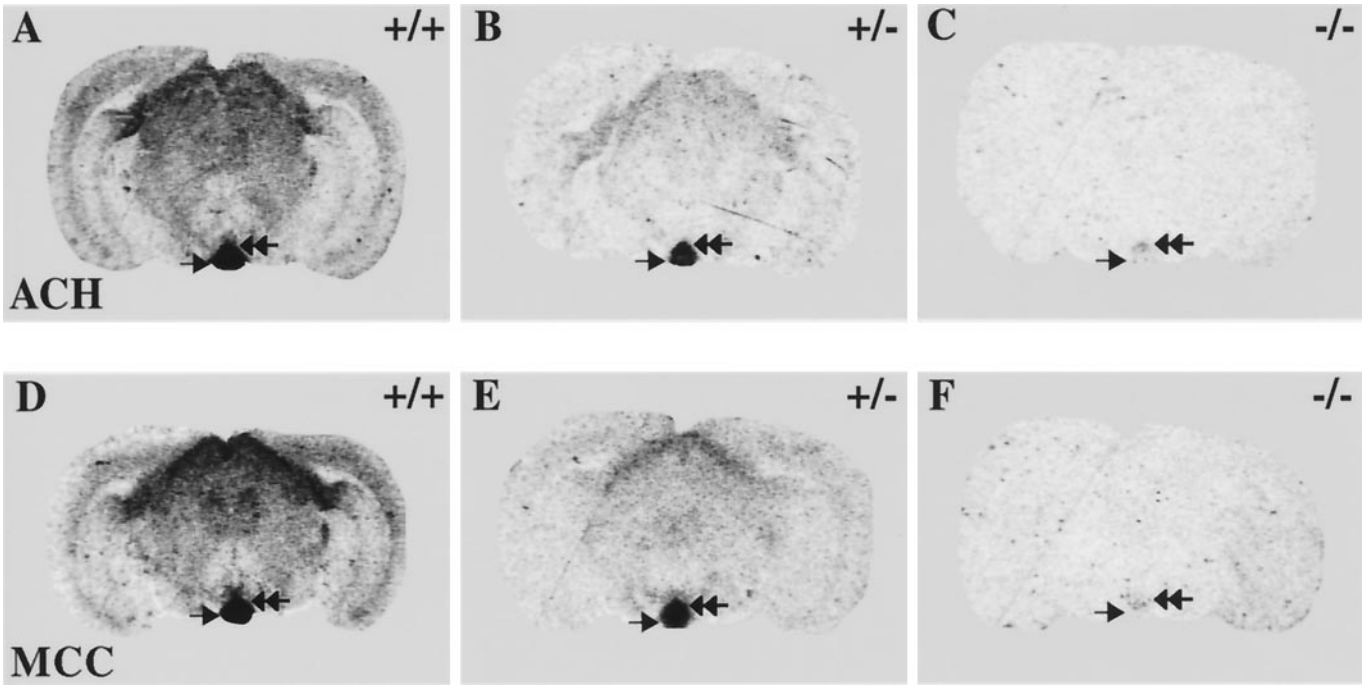

Figure 3. Film autoradiograms of ^{3}H-methylcarbamylcholine and ^{3}H-acetylcholine binding at bregma level −3.4 mm of β2 +/+, +/−, and −/− mice. The *arrow* and *double arrow* indicate the ventral and dorsal interpeduncular nucleus, respectively. Both ligands show persisting binding in the dorsal portion of the interpeduncular nucleus of β2 −/− mice. *ACH*, Acetylcholine; *MCC*, methylcarbamylcholine.

olis, IN) and following the specifications of the manufacturer to a specific activity of 100–300 kBq/pmol. The labeled probes were separated from unincorporated ^{35}S-dATP by using NucTrap push columns (Stratagene, La Jolla, CA), precipitated in ethanol, and resuspended in distilled water containing 50 mM dithiothreitol.

Frozen tissues from two rat and two mouse brains were cut at the cryostat (14-μm-thick sections) at level −13.8 and −7.5 mm, respectively, thaw-mounted on poly-L-lysine-coated slides, and stored at −80°C for 1–3 d. The procedure was performed according to Zoli et al. (1995). Probes were applied at a concentration of 2000–3000 Bq per 30 μl/section (corresponding to ~15 fmol/section). The slides were exposed for 7 d to ^{3}H-Hyperfilm (Amersham).

Patch clamp in brain sections

Preparation of the slices and solutions. The 6- to 15-d-old mice were anesthetized with ether and decapitated; brains were removed and placed in ice-cold Krebs' solution containing (in mM) 126 NaCl, 26 $NaHCO_3$, 25 glucose, 1.25 NaH_2PO_4, 2.5 KCl, 2 $CaCl_2$, and 1 $MgCl_2$ bubbled with 95% O_2/5% CO_2. Slices (300 μM thick) were obtained by using a DSK-1000 slicer (Dosaka, Japan) and were kept submerged on a net in 200 ml of Krebs' solution. Recordings were performed under an Axioscop microscope (Zeiss, Oberkochen, Germany). The neurons could be visualized easily without the help of phase-contrast optics. Drugs were applied either in the bath or with a broken patch pipette (tip ≈50 μm diameter) placed at the surface of the slice; this pipette allowed for either an outward flow of drug or an inward flow of extracellular medium. This system exchanged solution close to the cell in the 1–5 sec range. As a result, fast desensitizing nAChR currents may have been missed. When applied through the pipette, the drugs were dissolved in (in mM) 150 NaCl, 10 HEPES, 2 $CaCl_2$, 1 $MgCl_2$, and 2.5 KCl, pH 7.3.

Electrophysiological recordings. The patch pipettes were pulled from thin hard glass tubes (Hilgenberg, Germany) with a P-87 Sutter Instruments puller, wax-coated, and filled with (in mM) 135 CsCl, 10 BAPTA, 10 HEPES, 5 $MgCl_2$, and 4 NaATP, pH 7.3, yielding a 2–3 MΩ resistance. Voltage-clamp experiments were performed with an Axopatch 1D amplifier (Axon Instruments, Foster City, CA). Gigaseals were obtained without cleaning the cells. Currents were acquired on a PC computer with the pCLAMP6 package (Axon Instruments). Episodes of drug application were interspaced by 15–45 min to allow the nAChRs to recover from desensitization.

RESULTS

Binding of neuronal nicotinic receptor ligands in normal adult mice

The distribution of ^{3}H-nicotine, ^{3}H-cytisine, ^{3}H-acetylcholine, ^{3}H-methylcarbamylcholine, and ^{3}H-epibatidine labeling in equilibrium binding experiments in section through the mouse brain tallies well with the distribution of these ligands in the rat brain (Clarke et al., 1985; Happe et al., 1994; Perry and Kellar, 1995; Aubert et al., 1996) as well as with previous studies in the mouse brain (Marks et al., 1992). The overall pattern of labeling of all of the neuronal nicotinic ligands used in this study was similar (Figs. 1–5). The highest level of binding was detected in thalamic nuclei, especially anterior nuclei, and the interpeduncular nucleus (IPn), especially its dorsal portion, whereas moderate levels were found in several brainstem nuclei. ^{3}H-Epibatidine binding partially differed from this general pattern, because, in addition to the labeling common to all of the other ligands, it was present at high levels in the medial habenula (MHb), fasciculus retroflexus (fr), ventral IPn, nucleus tractus solitarii (Sol), area postrema (AP), and dorsal motor nucleus of the vagus nerve (DMnX). Accordingly, quantitative analysis of the autoradiograms revealed that the ratio of ^{3}H-epibatidine to ^{3}H-cytisine binding, at the concentration and specific activity of the ligands used in the present experiment, was between 1.5 and 2 in most brain areas of wild-type mice, but the ratio reached 10 in the medial part of MHb, 6.5 in the lateral part of MHb, 4 in the ventral IPn and fr, 6.5 in the Sol/DMnX, and 19 in the AP (Table 1). Notably, all areas with a ^{3}H-epibatidine/^{3}H-cytisine binding >2 displayed residual binding in β2 −/− mice (see below), with the exception of the superior colliculus (SC), which had a ratio of 2.5 but no residual binding. In view of the large number of nAChR subunits (including β2) expressed in the

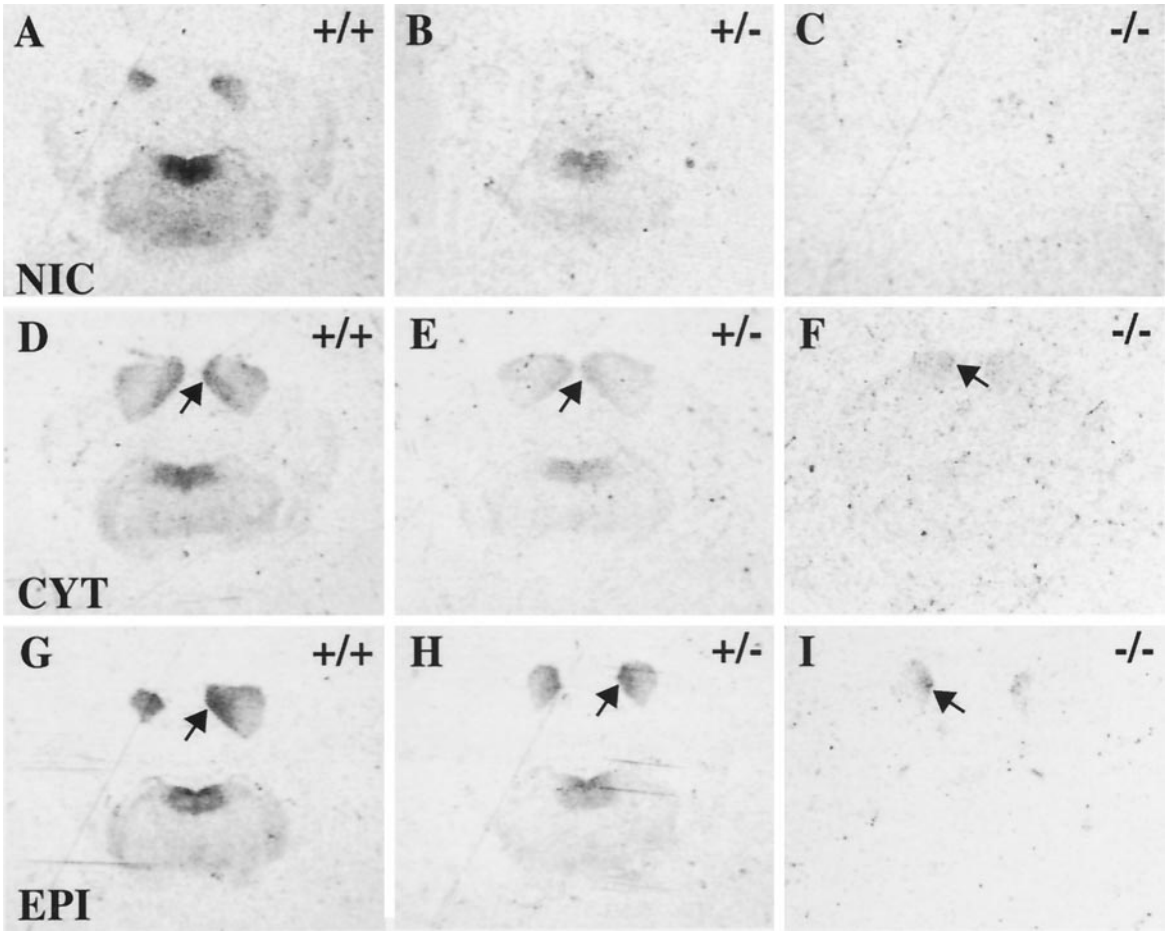

Figure 4. Film autoradiograms of ^{3}H-nicotine, ^{3}H-cytisine, and ^{3}H-epibatidine binding at bregma level −5.3 mm of β2 +/+, +/−, and −/− mice. The *arrow* indicates the dorsal cortex of the inferior colliculus. Both ^{3}H-cytisine and ^{3}H-epibatidine binding persist in this area. For abbreviations, see the legend to Figure 1.

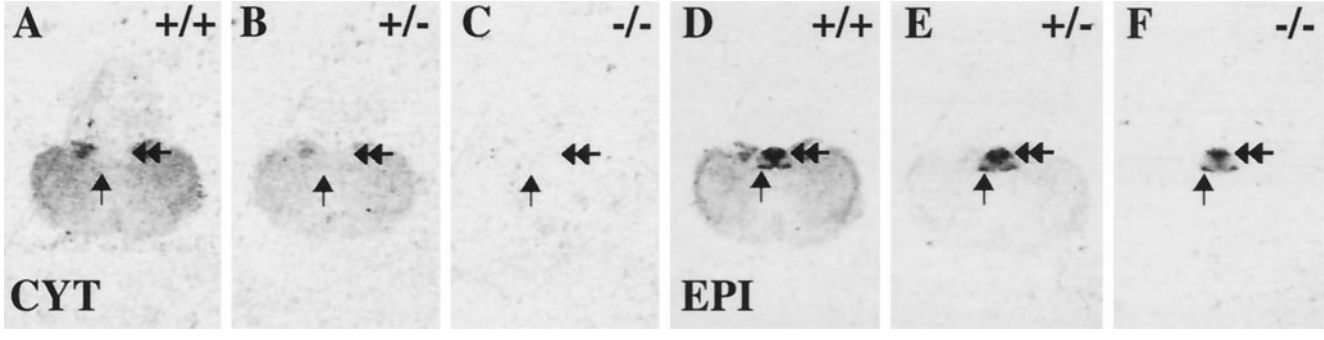

Figure 5. Film autoradiograms of ^{3}H-nicotine, ^{3}H-cytisine, and ^{3}H-epibatidine binding at bregma level −7.5 mm of β2 +/+, +/−, and −/− mice. The *arrow* and *double arrow* indicate the dorsal motor nucleus of the vagus nerve and the area postrema, respectively. Only ^{3}H-epibatidine binding persists in these nuclei of β2 −/− mice. For abbreviations, see the legend to Figure 1.

retina, which sends major afferents to the SC, it is possible that multiple β2-containing nAChR isotypes were detected here.

Binding of neuronal nicotinic receptor ligands in β2 −/− mice

As described previously (Picciotto et al., 1995), high-affinity binding of ^{3}H-nicotine was no longer detected in the brains of homozygous mice lacking the β2 subunit of the nAChR and was diminished by ~50% in the brains of mice heterozygous for this mutation (data not shown) (see Picciotto et al., 1995). This was also the case for the other nicotinic ligands tested in most brain areas containing detectable levels of nicotine binding in wild-type animals (Figs. 1–5). Binding of ^{3}H-epibatidine, ^{3}H-cytisine, ^{3}H-acetylcholine, and ^{3}H-methylcarbamylcholine persisted in a few well defined brain areas, however. The areas with residual binding for one or more of these ligands were the dorsal and ventral parts of the IPn, the MHb, the fr, the dorsal cortex of the inferior colliculus (DCIC), the dorsal tegmentum of the rostral medulla oblongata (DTgm), mainly corresponding to the medial and su-

Table 1. Quantitative analysis of ^{3}H-cytisine and ^{3}H-epibatidine binding in β2 +/+ mice

Brain area	^{3}H-cytisine	^{3}H-epibatidine	Ratio
Cg	1.03 ± 0.10	1.69 ± 0.01	1.6
Cx	0.91 ± 0.09	1.47 ± 0.07	1.6
CPu	1.03 ± 0.08	1.83 ± 0.09	1.8
Th	2.36 ± 0.21	4.16 ± 0.29	1.8
MHbm	1.76 ± 0.08	17.33 ± 1.55	**9.8**
MHbl	2.72 ± 0.14	17.33 ± 1.55	**6.4**
SC	1.89 ± 0.19	4.77 ± 0.06	2.5
fr	1.43 ± 0.11	5.53 ± 0.35	**3.9**
IPnd	7.52 ± 0.44	18.99 ± 0.71	**2.5**
IPnv	5.11 ± 0.13	19.97 ± 0.03	**3.9**
DCIC	0.88 ± 0.11	2.58 ± 0.06	**2.9**
DTgp	1.69 ± 0.13	3.13 ± 0.05	1.8
DTgm	0.74 ± 0.05	1.77 ± 0.11	**2.4**
7	0.50 ± 0.06	0.89 ± 0.05	1.8
AP	0.34 ± 0.05	5.50 ± 0.30	**16.2**
Sol	0.66 ± 0.05	4.17 ± 0.20	**6.3**

Mean values ± SEM are expressed as fmol/mg prot. The ratio between ^{3}H-epibatidine and ^{3}H-cytisine binding is given also. Areas in which some residual binding was observed in β2 −/− mice are highlighted.

7, Motor nucleus of the facial nerve; AP, area postrema; Cg, cingulate cortex; CPu, caudate putamen; Cx, cerebral cortex; DCIC, dorsal cortex of the inferior colliculus; DTgm, dorsal tegmentum of the medulla oblongata; DTgp, dorsal tegmentum of the pons; IPnd, interpeduncular nucleus, dorsal part; IPnv, interpeduncular nucleus, ventral part; MHbl, medial habenula, lateral part; MHbm, medial habenula, medial part; SC, superior colliculus; Sol, nucleus tractus solitarii; Th, thalamic nuclei.

perior vestibular nuclei, the AP, the Sol, and the DMnX (Figs. 1–5). When the sections were exposed for 4 months, in two of five brains of β2 −/− mice faint binding for ^{3}H-epibatidine also was detected in the medial rim of the amygdala (mAmy), the brachium of the inferior colliculus (bic), and the laterodorsal tegmental nucleus of the pons (LDTg). Binding was absent or greatly reduced (in the areas with the highest labeling) in all of these areas when the ligands were incubated in the presence of 10 μM cold nicotine.

In β2 −/− mice, ^{3}H-epibatidine was detected at high levels in dorsal and ventral IPn, MHb, fr, AP, and DMnX; at low levels in DCIC, DTgm, and Sol (Figs. 1, 2, 4, 5); and was barely detectable in mAmy, bic, and LDTg. Quantitative analysis showed that approximately the same amount of ^{3}H-epibatidine binding in IPn, MHb, fr, AP, Sol, and DMnX was present in wild-type and mutant mice (Fig. 6), demonstrating that the vast majority of ^{3}H-epibatidine binding in wild-type mice in these areas results from nAChRs that do not contain the β2 subunit. Instead, in DCIC and DTgm, ^{3}H-epibatidine binding to nAChRs containing β2 subunit was predominant (60–70% of the total ^{3}H-epibatidine binding) (Fig. 6). Because the affinity of ^{3}H-epibatidine for β2-containing and non-β2-containing nAChR isoforms was not determined in the present experiments, it was not possible to know whether the amount of ^{3}H-epibatidine binding that was left in mutants accurately reflected the number of binding sites (see Discussion).

^{3}H-Cytisine had a distribution in mutant mice similar to that of ^{3}H-epibatidine, with the exception of the total absence of labeling in AP, Sol, and DMnX (Figs. 5, 6). In addition, contrary to ^{3}H-epibatidine, only faint labeling was observed in ventral IPn and medial MHb in mutant mice (see Figs. 1, 2, 6).

In mutant mice, ^{3}H-methylcarbamylcholine and ^{3}H-acetylcholine were detected but at a low level in the dorsal IPn (see Fig. 3).

^{125}I-α-Bungarotoxin binding in β2 −/− mice

Overall, the pattern of ^{125}I-α-bungarotoxin binding did not differ substantially in β2 +/+, +/−, and −/− mice. A quantitative analysis of the autoradiographs did not reveal significant region-specific differences in the level of α-bungarotoxin binding in the brains of β2 mutant mice as compared with their wild-type siblings (Fig. 6).

Binding of muscarinic ligands in β2 −/− mice

In agreement with previous reports, in wild-type mice the ^{3}H-pirenzepine binding was concentrated selectively in telencephalic areas, namely neocortex, hippocampal formation, and striatum, whereas ^{3}H-AF-DX384 was present at high levels in most gray matter areas. These patterns of binding persisted in β2 −/− mice. The quantitative analysis performed in neocortex (M1 and M2), cingulate cortex (M1 and M2), caudate-putamen (M1 and M2), olfactory tubercle (M1 and M2), medial septum (M2), CA1 and CA3 hippocampal fields (M1 and M2), dentate gyrus (M1 and M2), central, dorsal, and ventral thalamus (M2), and hypothalamus (M2) confirmed that no significant difference was present in the areas analyzed (data not shown) for both ligands between β2 −/− mice and their wild-type or heterozygous siblings.

Localization of nicotinic subunit mRNAs in the dorsocaudal medulla oblongata

The autoradiographic study described above shows that high levels of ^{3}H-epibatidine binding persist in some nuclei of the dorsocaudal medulla oblongata of mutant mice. Previous *in situ* hybridization studies of nAChR subunit distribution in this area showed the presence of relatively high levels of α3 and α5 mRNAs but only low (α4, and β2) to undetectable (α2, α6, and β3) levels of other subunits (Wada et al., 1989, 1990; Le Novère et al., 1996). No information is available on β4 mRNA in this region. We therefore studied the distribution of α3, α5, and β4 mRNAs in the caudal medulla oblongata of both rat and mouse brains by using *in situ* hybridization histochemistry and compared it with ^{3}H-epibatidine binding in the same region. The distribution of α3 and β4 mRNAs was the same. In the rat caudodorsal medulla oblongata the labeling was rather homogeneous over the AP, Sol, and DMnX (Fig. 7). In the mouse the labeling appeared more heterogeneous, being high in the DMnX, moderate in the AP, and low in the Sol (Fig. 8). This pattern closely resembled that of ^{3}H-epibatidine in the same areas in both animal species. α5 mRNA labeling was fainter than the labeling of α3 and β4 mRNAs and barely visible in the dorsocaudal medulla oblongata of the mouse.

Electrophysiological analysis of nicotinic receptors in the thalamus, medial habenula, interpeduncular nucleus, and dorsal motor nucleus of the vagus nerve

We next attempted to correlate the binding activity with the electrophysiological responses to various nicotinic agonists in a slice preparation of mouse brain. The slice preparation allowed for the accurate localization of the neurons but precluded a fast application of the agonists because of the slow diffusion of the drugs into the slice. In wild-type mice we tested neurons in the anterior group of the thalamus that express a very high level of high-affinity nicotine binding sites in wild-type mice. We found that micromolar concentrations of nicotine elicited responses larger than those elicited by DMPP and that cytisine was a poor

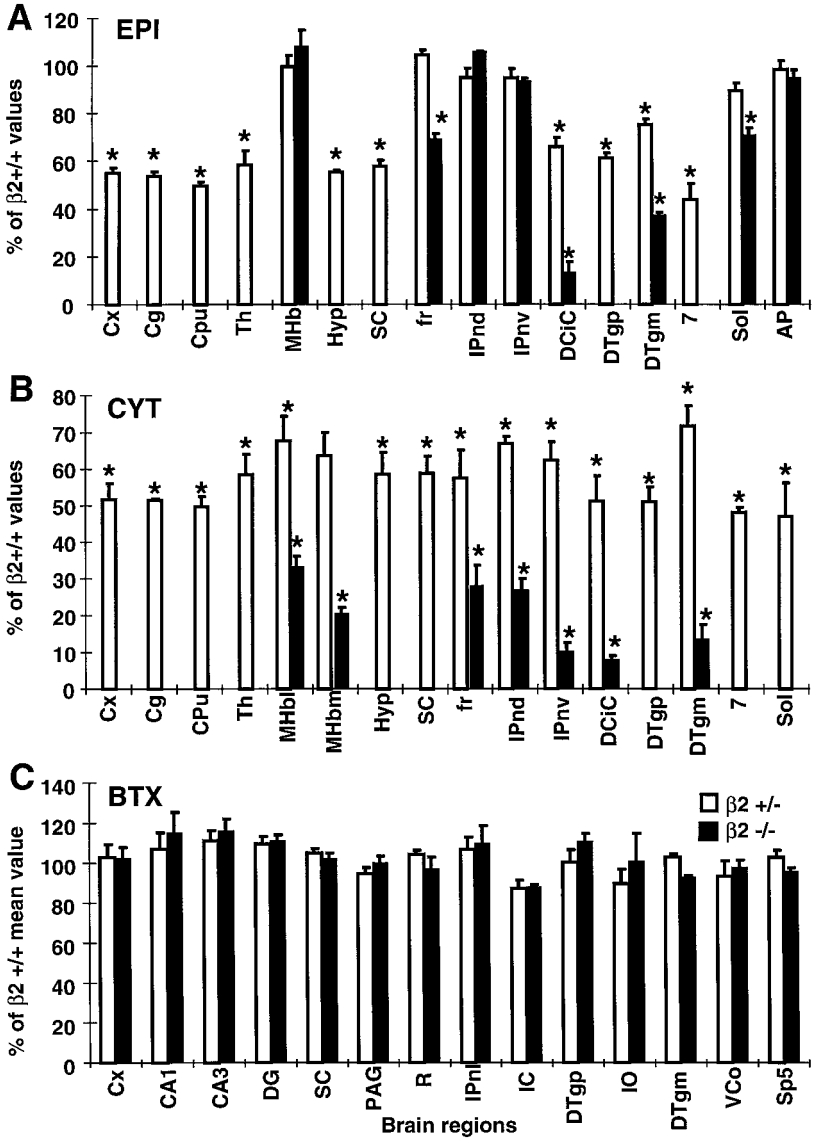

Figure 6. Quantitative analysis of ^{3}H-epibatidine (*EPI* in *A*), ^{3}H-cytisine (*CYT* in *B*), and ^{125}I-α-bungarotoxin (*BTX* in *C*) binding in β2 +/− and −/− mice. The results are expressed as the mean percentage values ± SEM of the respective +/+ mean value. Statistical analysis according to Mann–Whitney *U* test; $^{*}p < 0.01$ versus β2 +/+ mean value. For abbreviations, see the legend to Table 1 plus the following: *CA1, CA3*, hippocampal fields CA1 and CA3; *DG*, dentate gyrus; *Hyp*, hypothalamus; *IC*, inferior colliculus; *IO*, inferior olive; *IPnl*, interpeduncular nucleus, lateral part; *PAG*, periaqueductal gray; *R*, red nucleus; *Sp5*, spinal trigeminal nucleus; *VCo*, ventral cochlear nucleus.

agonist in the thalamus (Fig. 9*A*). Epibatidine was a potent agonist at concentrations above 10 nM. The responses to nicotine were blocked by 1 μM DHβE and 10 μM MCA, but not by 5 nM MLA (Fig. 10), an antagonist that completely blocks the response of α-bungarotoxin-sensitive nAChRs at a dose of 1 nM in cultures of hippocampal neurons (Alkondon and Albuquerque, 1993). No nicotinic response persisted in the thalamus of mutant mice (Picciotto et al., 1995), demonstrating the necessary contribution of the β2 subunit to functional nAChRs in the thalamus. Other areas with similar binding features (disappearance of every type of nicotinic agonist binding in mutant mice), such as the substantia nigra and ventral tegmental area, also showed a similar pharmacological spectrum in wild-type mice (nicotine ≫ cytisine) and the disappearance of the response in mutant mice (Picciotto et al., 1998).

We then investigated the nicotinic responses in brain areas in which high levels of binding remained in mice lacking the β2 subunit. Responses could be recorded in the structures expressing high-affinity binding sites for epibatidine alone (ventral MHb, DMnX) or for epibatidine and cytisine (dorsal IPn) in the mutant mice (small nicotinic responses also were observed in four of nine cells in the DCIC, but no pharmacological investigation was undertaken in this structure). In the MHb, the DMnX, and the IPn we found a similar activity of cytisine, nicotine, and DMPP in the micromolar range (see Fig. 9*B–D*). The sensitivity to nicotine was slightly higher than that reported in the rat DMnX (Bertolino et al., 1997). Epibatidine elicited large currents at concentrations above 10 nM. When recorded in neurons from the MHb and IPn of wild-type mice, the amplitude of responses to 10 μM nicotine, DMPP, and cytisine and the relative potency of these agonists were similar to those observed in mutant mice (Picciotto et al., 1995) (data not shown). Thus, the contribution of β2-containing nAChRs to the nicotinic responses recorded in our preparations of the IPn and MHb is minimal in wild-type mice. Nicotinic responses were blocked by 1 μM MCA, but not by 5 nM MLA in both MHb and IPn, whereas 1 μM DHβE reduced the nicotinic responses in the IPn, but not in the MHb, indicating a difference between the nAChRs in the two structures (Fig. 10) (Mulle et al., 1991). nAChRs recorded in β2 −/− MHb and IPn also differed with regard to the desensitization time constant of the responses to high concentrations of nicotinic ago-

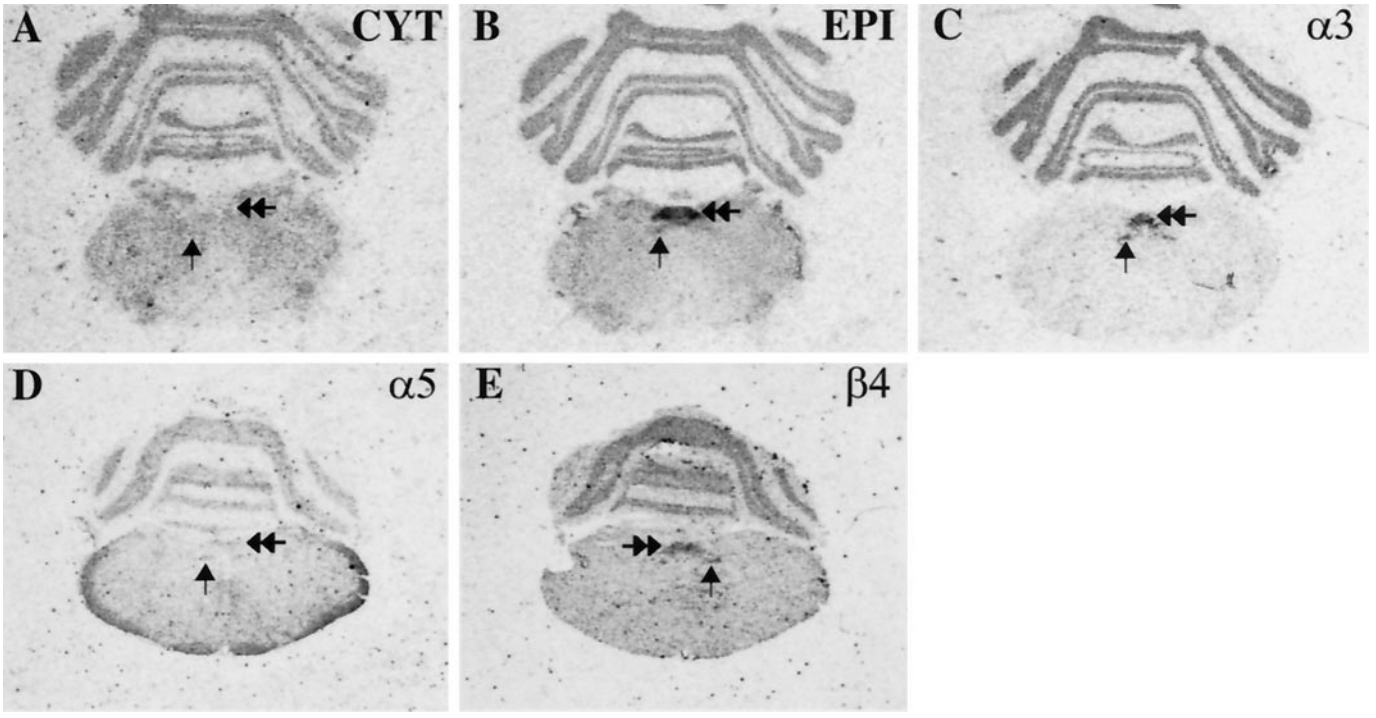

Figure 7. Film autoradiograms of ^{3}H-cytisine and ^{3}H-epibatidine binding and α3, α5, and β4 mRNA levels at bregma level −13.8 mm of adult rats. The *arrow* and *double arrow* indicate the dorsal motor nucleus of the vagus nerve and the area postrema, respectively. For abbreviations, see the legend to Figure 1.

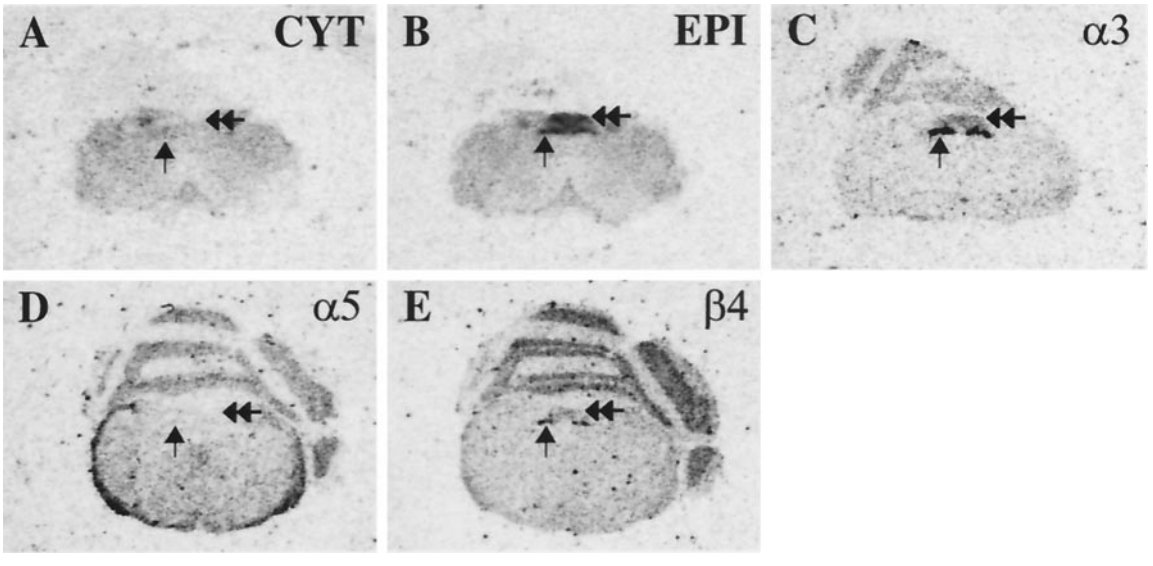

Figure 8. Film autoradiograms of ^{3}H-cytisine and ^{3}H-epibatidine binding and α3, α5, and β4 mRNA levels at bregma level −7.5 mm of adult mice. The *arrow* and *double arrow* indicate the dorsal motor nucleus of the vagus nerve and the area postrema, respectively. For abbreviations, see the legend to Figure 1.

nists (mean ± SD for 100 μM nicotine: 4.16 ± 1.13 sec, $n = 4$, in the IPn; 20.0 ± 7.34 sec, $n = 5$, in the MHb) (Fig. 11).

DISCUSSION

Contrary to what is assumed normally, nicotinic agonists bind with high affinity to different nAChRs in equilibrium binding experiments, including some nAChRs that do not contain β2. Instead, muscarinic receptors remained unchanged in the brain of mutant mice, confirming that the mutation of a nicotinic subunit specifically affects the nicotinic cholinergic system. The findings in this study, together with previous experiments on the anatomy and electrophysiology of nAChRs, allow us to propose an extension of the classification of brain nAChRs (Alkondon and Albuquerque, 1993) (Table 2).

Different spectra of high-affinity binding and electrophysiological responses of neuronal nicotinic ligands for nAChR isotypes

At least four groups of nAChR isotypes can be identified on the basis of the present data.

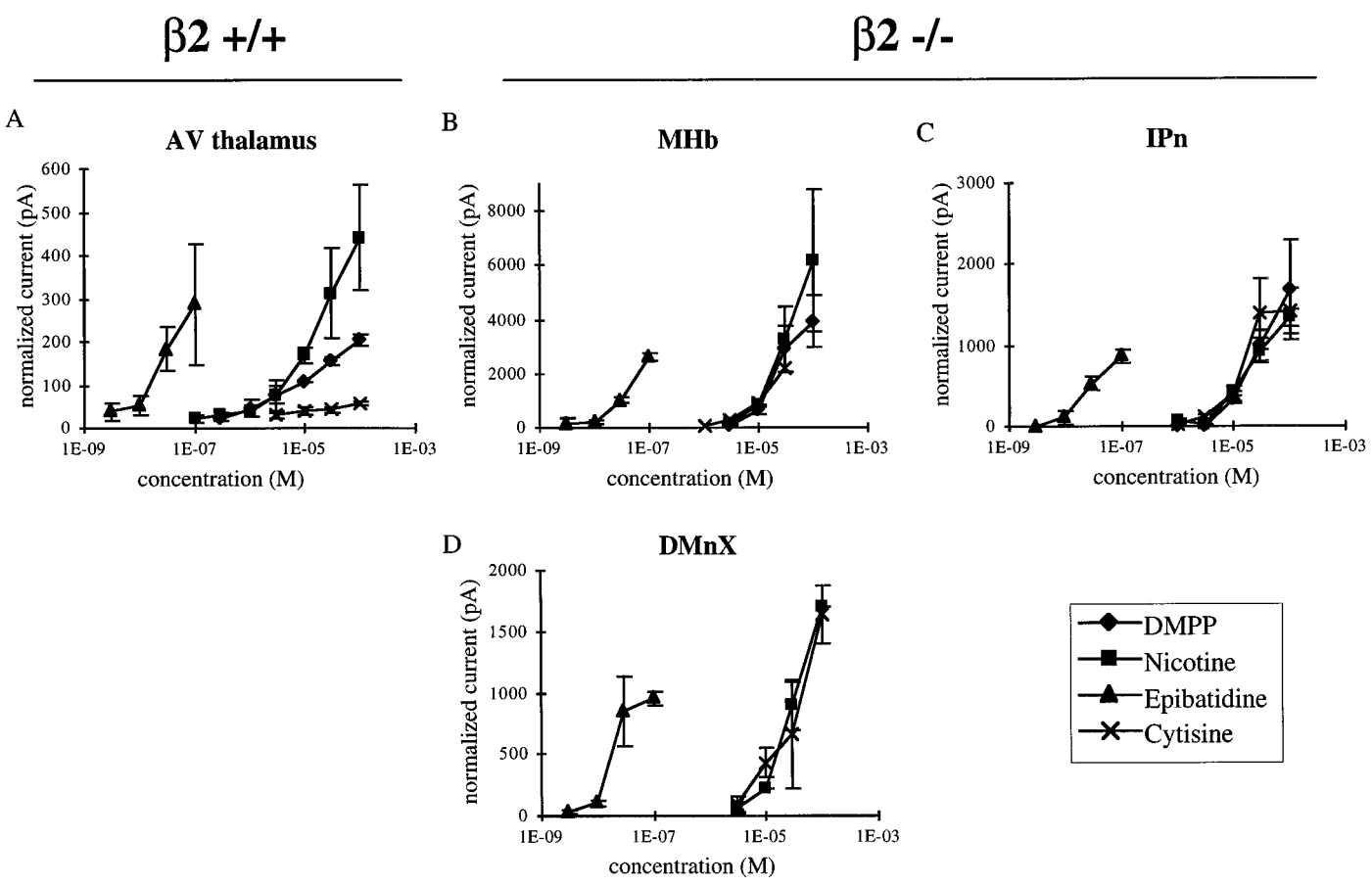

Figure 9. Dose–response curve for epibatidine, nicotine, cytisine, and DMPP in the brain of β2 +/+ and β2 −/− mice. *A*, Antero-ventral (AV) thalamus of β2 +/+ mice. *B–D*, Other brain regions of β2 −/− mice: ventromedial MHb (*B*), (antero-) dorsal IPn (*C*), and DMnX (*D*). Each *point* is the mean ± SEM of 2–12 measures. Normalization between different cells was performed with responses to 10 μM DMPP in the thalamus and to 10 μM nicotine in the other structures. Then the normalized currents were multiplied by the average amplitude of the responses to 10 μM nicotine and DMPP. Note the smaller amplitude of responses in the thalamus as compared with other structures. We have recorded 51 cells in the thalamus, 31 cells in the MHb, 13 cells in the DMnX, and 40 cells in the IPn. The average number of different conditions tested per cell is 4.5.

Type 1 nAChRs are α-bungarotoxin-sensitive and have low affinity for neuronal nicotinic agonists in equilibrium binding experiments. Their distribution does not change significantly in β2 −/− mice, whereas their disappearance in α7 mutant mice (Orr-Utreger et al., 1997) confirms that they contain the α7 subunit and that the β2 subunit is not a component.

Type 2 nAChRs contain the β2 subunit and represent the vast majority of nAChRs in the mouse brain. The order of agonist potency for this type of nAChR is consistent with *in vitro* expression of α4/β2 (Luetje and Patrick, 1991). Cytisine is a poor agonist for β2-containing nAChRs in the dopaminergic system (Picciotto et al., 1998) and in cultured hippocampal neurons (Alkondon and Albuquerque, 1993), indicating that this is a characteristic property of type 2 nAChRs. Type 2 nAChRs are present at high levels in the thalamus and the habenulo-interpeduncular system, especially the IPn. All nicotinic ligands used in the present study are able to bind this group of isotypes with nanomolar or subnanomolar (^{3}H-epibatidine) K_D in equilibrium binding experiments. In contrast to the other ligands that were used, high-affinity ^{3}H-nicotine binding completely disappears in β2 −/− animals and can be considered a marker of this group of nAChRs. By comparing the present results with previous localization studies, it follows that the composition of the major isoform constituting type 2 binding is α4/β2.

Other subunits are likely to coassemble with β2, namely, α2 and α3, α5 as a third subunit (Vernallis et al., 1993; Wang et al., 1996), and β4 as a fourth subunit (Conroy and Berg, 1995). An α2/β2 isoform likely contributes to type 2 binding because α2, more than α4, is concentrated in the IPn, which contains the highest level of ^{3}H-nicotine binding in the brain. It is difficult to ascertain from our results if α3/β2 contributes to type 2 binding in some areas of the mouse brain. The highest levels of α3 are distributed homogeneously in the ventral portion of the MHb (Wada et al., 1989; Le Novère et al., 1996). The subnuclear distribution of ^{3}H-nicotine in the MHb (higher in the lateral than in the medial part) suggests that, at least in this nucleus, α3 does not contribute substantially to type 2 binding. α6 and β3 mRNAs are enriched in the dopaminergic neurons of the ventral mesencephalon and the noradrenergic neurons of the locus coeruleus (Le Novère et al., 1996). Electrophysiological experiments did not reveal any response to nicotinic agonists in the dopaminergic neurons of the ventral mesencephalon of β2 −/− mice (Picciotto et al., 1998), suggesting that in this area the nAChRs, which putatively contain α6 and β3, also contain the β2 subunit.

Type 3 nAChRs do not contain β2 and bind only ^{3}H-epibatidine with high affinity in equilibrium binding experiments. This isotype was clearly identified in the dorsocaudal medulla oblongata (Sol, DMnX, and AP), in the pineal gland (M. Zoli, unpublished

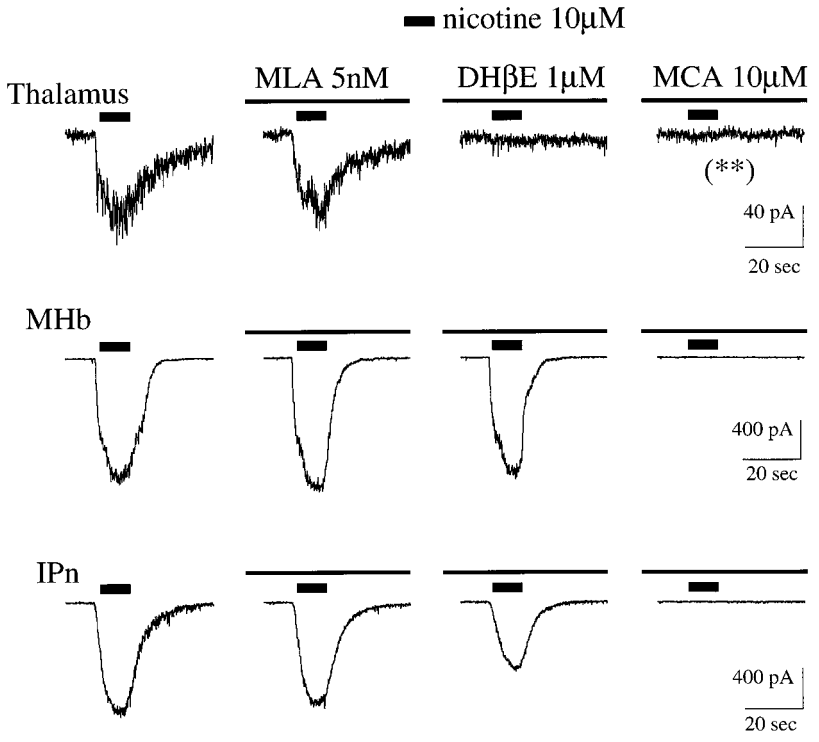

Figure 10. Differential sensitivity to the nicotinic antagonists methyllycaconitine (*MLA*), dihydro-β-erythroidine (*DHβE*), and mecamylamine (*MCA*) of the nicotinic responses in the thalamus of β2 +/+ mice and in the MHb and IPn of β2 −/− mice. The antagonists were applied 5–10 min before (and during) the application of nicotine. MLA (5 nM) had little effect on the nicotinic responses, whereas 10 μM mecamylamine totally abolished the nicotinic responses to 10 μM nicotine. The responses were totally inhibited by 1 μM DHβE in the wild-type thalamus, partially inhibited in the mutant interpeduncular nucleus (*IPn*), and not inhibited in the mutant medial habenula (*MHb*). (**), MCA application and MLA and DHbE applications were performed in two different thalamic neurons with similar control response to 10 μM DMPP.

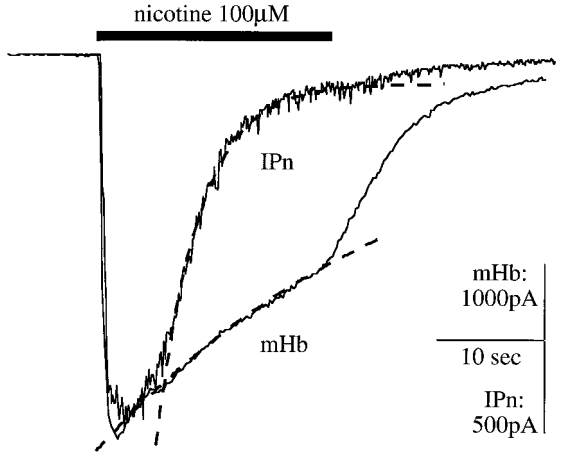

Figure 11. Desensitization of nicotinic responses in the IPn and MHb of β2 −/− mice. The responses to 100 μM nicotine in the medial habenula and in the interpeduncular nucleus have been normalized. The decay of the responses was fit by a single exponential function (*dashed line*). In the cells shown, the desensitization time constant of the responses was 30.0 sec (*MHb*) and 3.95 sec (*IPn*).

data), and in the habenulo-interpeduncular system, where it was transported from the MHb to the IPn. ^{3}H-Epibatidine binding did not decrease significantly in MHb (especially its medial portion), fr, and ventral IPn in β2 mutant mice. The ratio of ^{3}H-epibatidine to ^{3}H-cytisine in MHb, fr, and ventral (but not dorsal) IPn in wild-type mice was higher than in other brain areas, except the dorsocaudal medulla oblongata, implying that these sites might have higher affinity for epibatidine than type 2 nAChRs. In preliminary experiments both type 2 and type 3 binding decreased in parallel when assayed with 0.02 and 0.002 nM ^{3}H-epibatidine (M. Zoli unpublished data), suggesting that their affinity for epibatidine was similar. Electrophysiological experiments in the MHb and DMnX of mutant mice showed an agonist potency consistent with α3/β4 nAChRs expressed in oocytes (Luetje and Patrick, 1991) (also see below) and a slow rate of desensitization. Although *in situ* hybridization studies (Wada et al., 1989; Hill et al., 1993), single channel recordings (Connolly et al., 1995), and binding studies indicate the presence of multiple subtypes of nAChRs in the MHb, present and previous (Picciotto et al., 1995) results point to the existence of a predominant subtype (a type 3 nAChR) in the MHb of both β2 +/+ and −/− mice.

Type 3 binding corresponds to the distribution of α3/β4 subunits that are coexpressed at high levels in MHb (Wada et al., 1989; Hill et al., 1993; Zoli et al., 1995), dorsocaudal medulla oblongata, and pineal gland (Zoli et al., 1995). On the basis of the expression pattern of α5, this subunit either is not a component of this receptor or does not change its binding characteristics.

Type 4 nAChRs do not contain β2 and bind ^{3}H-epibatidine and ^{3}H-cytisine with high affinity in equilibrium binding experiments. The binding of other nicotinic ligands is very limited (^{3}H-methylcarbamylcholine and ^{3}H-acetylcholine) or is absent (^{3}H-nicotine). This isotype or isotypes were found in the DCIC, DTgm, and the habenulo-interpeduncular system, where they could be detected in the MHb (especially laterally), IPn (especially dorsally), and fr, implying that this isotype or isotypes are, at least in part, transported from the MHb to the IPn. Electrophysiological experiments in the dorsal IPn showed an order of potency of agonists consistent with a β4-containing receptor (Luetje and Patrick, 1991). Currents elicited by high concentrations of nicotinic agonists in the dorsal IPn (type 4 nAChRs) exhibited a substantially faster desensitization than those in the MHb (type 3 nAChRs). The known distribution of nAChR subunits does not allow for the unequivocal identification of the subunit composition of this receptor or receptors. The putative composition of type 4 nAChRs in intrinsic neurons of the IPn may be α2 and/or α4 with β4. The heterogeneous distribution of ^{3}H-cytisine binding in the MHb of β2 −/− mice fits well with the

Table 2. Proposed classification of nAChRs in the mouse brain

Receptor class	Putative composition	Predominant localization in CNS	High-affinity binding at equilibrium	Pharmacology in slices
Type 1	α7	Cortex and limbic areas	αBTX	αBTX and MLA-sensitive, very fast desensitization
Type 2	β2-α4-(α5?) β2-(α2?) β2-(α3?) β2-(α6-β3?)	All CNS IPn Hippocampus Catecholaminergic nuclei	EPI > NIC = CYT = MCC = ACH	MLA-insensitive, NIC ≫ CYT, DHβE = MCA
Type 3	β4-α3-(α5?)	MHb, IPn, dorsal medulla	EPI	MLA-insensitive, CYT = NIC, DHβE < MCA slow decay at 100 μM NICO
Type 4	(β4-α4?) (β4-α2?)	Lateral MHb Dorsal IPn	EPI > CYT > MCC = ACH	MLA-insensitive, CYT = NIC, DHβE < MCA fast decay at 100 μM NICO

ACH, Acetylcholine; αBTX, α-bungarotoxin; MCC, methylcarbamylcholine; CYT, cytisine; DHβE, dihydro-β-erythroidine; EPI, epibatidine; IPn, interpeduncular nucleus; MCA, mecamylamine; MHb, medial habenula; MLA, methyllycaconitine; NIC, nicotine.

distribution of α4 and α5 (Wada et al., 1989; Le Novère et al., 1996). It therefore is possible that receptors composed of α4/β4 (with or without α5) and/or α3/α5/β4 account for type 4 binding in the MHb.

Differences between affinity in equilibrium binding and in electrophysiological experiments

The equilibrium binding constants for cytisine, nicotine, and epibatidine in binding experiments are below 10 nM, 10 nM, and 500 pM, respectively (Romano and Goldstein, 1980; Pabreza et al., 1991; Houghtling et al., 1995), but at these concentrations none of these agonists activates a significant current in our study. The active state is detected readily in electrophysiological experiments, whereas the desensitized states have higher affinities for the agonists, are more stable in the presence of agonist, and therefore are detected in equilibrium binding experiments. There is also a lack of correspondence between the order of potency of agonists in electrophysiological experiments and their affinity in equilibrium binding experiments. For instance, the type 2 nAChRs have a very similar K_D for nicotine and cytisine, whereas the order of potency is nicotine ≫ cytisine in electrophysiological experiments. Similar disparities can be seen for types 3 and 4 nAChRs. This may be attributable to the fact that the desensitized states (equilibrium binding) and the active states (electrophysiological experiments) do not share the same affinity for these ligands, as has been demonstrated already in the case of the muscle nAChR (Changeux, 1990). Receptor autoradiography only recognizes high-affinity binding at equilibrium so that some nAChRs isoforms may not have been detected in binding experiments. In addition, electrophysiological data are pooled and averaged for many cells so that the dose–response curves presented account only for the behavior of the main subtype present in the cells. Minor populations of nAChRs thus may have been missed by both techniques.

Conclusions

These experiments demonstrate that there are at least four classes of nAChRs in the brain, which can be distinguished on the basis of their distribution, high-affinity binding characteristics, and response to nicotinic agonists in electrophysiological experiments; the classification provides a tentative identification of the subunit composition of these subtypes. Future experiments that use knock-out animals lacking individual α subunits should allow for a further dissection of the subunit composition of these receptors.

REFERENCES

Alkondon M, Albuquerque EX (1993) Diversity of nicotinic acetylcholine receptors in rat hippocampal neurons. I. Pharmacological and functional evidence for distinct structural subtypes. J Pharmacol Exp Ther 265:1455–1473.

Alkondon M, Reinhardt S, Lobron C, Hermsen B, Maelicke A, Albuquerque EX (1994) Diversity of nicotinic acetylcholine receptors in rat hippocampal neurons. II. The rundown and inward rectification of agonist-elicited whole-cell currents and identification of receptor subunits by *in situ* hybridization. J Pharmacol Exp Ther 271:494–506.

Aubert I, Cecyre D, Gauthier S, Quirion R (1996) Comparative ontogenic profile of cholinergic markers, including nicotinic and muscarinic receptors, in the rat brain. J Comp Neurol 369:31–55.

Badio B, Daly JW (1994) Epibatidine, a potent analgetic and nicotinic agonist. Mol Pharmacol 45:563–569.

Benfenati F, Cimino M, Agnati LF, Fuxe K (1986) Quantitative autoradiography of central neurotransmitter receptors: methodological and statistical aspects with special reference to computer-assisted image analysis. Acta Physiol Scand 128:129–146.

Bertolino M, Kellar KJ, Vicini C, Gillis RA (1997) Nicotinic receptor mediates spontaneous GABA release in the rat dorsal motor nucleus of the vagus. Neuroscience 79:671–681.

Changeux JP (1990) Functional architecture and dynamics of the nicotinic acetylcholine receptor: an allosteric ligand-gated ion channel. In: Fidia Research Foundation neuroscience award lectures, Vol 4 (Llinás RR, Bloom FE, eds) pp 21–168. New York: Raven.

Clarke PBS, Schwartz RD, Paul SM, Pert CB, Pert A (1985) Nicotinic binding in rat brain: autoradiographic comparison of [^{3}H]acetylcholine, [^{3}H]nicotine, and [^{125}I]-α-bungarotoxin. J Neurosci 5:1307–1315.

Connolly JG, Gibb AJ, Colquhoun D (1995) Heterogeneity of neuronal nicotinic acetylcholine receptors in thin slices of rat medial habenula. J Physiol (Lond) 484:87–105.

Conroy WG, Berg DK (1995) Neurons can maintain multiple classes of nicotinic acetylcholine receptors distinguished by different subunit compositions. J Biol Chem 270:4424–4431.

Cortes R, Probst A, Tobler HJ, Palacios JM (1986) Muscarinic cholinergic receptor subtypes in the human brain. II. Quantitative autoradiographic studies. Brain Res 362:239–253.

Couturier S, Bertrand D, Matter J-M, Hernandez M-C, Bertrand S, Millar N, Valera S, Barkas T, Ballivet M (1990) A neural nicotinic acetylcho

line receptor subunit (α7) is developmentally regulated and forms a homo-oligomeric channel blocked by α-BTX. Neuron 5:847–856.
Dineley-Miller K, Patrick J (1992) Gene transcripts for the nicotinic acetylcholine receptor subunit β4 are distributed in multiple areas of the rat central nervous system. Mol Brain Res 16:339–344.
Elgoyhen AB, Johnson DS, Boulter J, Vetter DE, Heinemann S (1994) α9: an acetylcholine receptor with novel pharmacological properties expressed in rat cochlear hair cells. Cell 79:705–715.
Fenster CP, Rains MF, Noerager B, Quick MW, Lester RAJ (1997) Influence of subunit composition on desensitization of neuronal acetylcholine receptors at low concentrations of nicotine. J Neurosci 17:5747–5759.
Franklin KBJ, Paxinos G (1997) The mouse brain in stereotaxic coordinates. New York: Academic.
Gerzanich V, Peng X, Wang F, Wells G, Anand R, Fletcher S, Lindstrom J (1995) Comparative pharmacology of epibatidine: a potent agonist for neuronal nicotinic acetylcholine receptors. Mol Pharmacol 48:774–782.
Happe HK, Peters JL, Bergman DA, Murrin LC (1994) Localization of nicotinic cholinergic receptors in rat brain: autoradiographic studies with ^{3}H-cytisine. Neuroscience 62:929–944.
Hill Jr JA, Zoli M, Bourgeois JP, Changeux JP (1993) Immunocytochemical localization of a neuronal nicotinic receptor: the β2 subunit. J Neurosci 13:1551–1568.
Houghtling RA, Davila-Garcia MI, Kellar KJ (1995) Characterization of (±)[^{3}H]epibatidine binding to nicotinic cholinergic receptors in rat and human brain. Mol Pharmacol 48:820–827.
Le Novère N, Changeux JP (1995) Molecular evolution of the nicotinic acetylcholine receptor: an example of multigene family in excitable cells. J Mol Evol 40:155–172.
Le Novère N, Zoli M, Changeux JP (1996) Neuronal nicotinic receptor α6 subunit mRNA is selectively concentrated in catecholaminergic nuclei of the rat brain. Eur J Neurosci 8:2428–2439.
Luetje CW, Patrick J (1991) Both α- and β-subunits contribute to the agonist sensitivity of neuronal nicotinic acetylcholine receptors. J Neurosci 11:837–845.
Marks MJ, Pauly JR, Gross SD, Deneris ES, Hermans-Borgmeyer I, Heinemann SF, Collins AC (1992) Nicotine binding and nicotinic receptor subunit mRNA after chronic nicotine treatment. J Neurosci 12:2765–2784.
Mulle C, Vidal C, Benoit P, Changeux JP (1991) Existence of different subtypes of nicotinic acetylcholine receptors in the rat habenulo-interpeduncular system. J Neurosci 11:2588–2597.
Orr-Utreger A, Goldner FM, Saeki M, Lorenzo I, Golberg L, De Biasi M, Dani JA, Patrick JW, Beaudet AL (1997) Mice deficient in the α7 neuronal nicotinic acetylcholine receptor lack α-bungarotoxin binding sites and hippocampal fast nicotinic currents. J Neurosci 17:9165–9171.
Pabreza LA, Dhawan S, Kellar KJ (1991) [^{3}H]Cytisine binding to nicotinic cholinergic receptors in brain. Mol Pharmacol 39:9–12.
Perry DC, Kellar KJ (1995) [^{3}H]Epibatidine labels nicotinic receptors in rat brain. An autoradiographic study. J Pharmacol Exp Ther 275:1030–1034.
Picciotto MR, Zoli M, Léna C, Bessis A, Lallemand Y, Le Novère N, Vincent P, Merlo Pich E, Brûlet P, Changeux JP (1995) Abnormal avoidance learning in mice lacking functional high-affinity nicotine receptor in the brain. Nature 374:65–67.
Picciotto MR, Zoli M, Rimondini R, Léna C, Marubio L, Merlo Pich E, Fuxe K, Changeux JP (1998) β2-Subunit-containing acetylcholine receptors are involved in the reinforcing properties of nicotine. Nature 391:173–176.
Regenold W, Araujo D, Quirion R (1987) Direct visualization of brain M2 muscarinic receptors using the selective antagonist [^{3}H]AF-DX116. Eur J Pharmacol 144:417–419.
Role LW, Berg DK (1996) Nicotinic receptors in the development and modulation of CNS synapses. Neuron 16:1077–1085.
Romano C, Goldstein A (1980) Stereospecific nicotine receptors on rat brain membranes. Science 210:647–650.
Sargent PB (1993) The diversity of neuronal nicotinic acetylcholine receptors. Annu Rev Neurosci 16:403–443.
Sullivan JP, Decker MW, Brioni JD, Donnelly-Roberts D, Anderson DJ, Bannon AW, Kang C, Adams P, Piattoni-Kaplan M, Buckley M, Gopalakrishnan M, Williams M, Arneric SP (1994) (±)Epibatidine elicits a diversity of *in vitro* and *in vivo* effects mediated by nicotinic acetylcholine receptors. J Pharmacol Exp Ther 271:624–631.
Vernallis AB, Conroy WG, Berg DK (1993) Neurons assemble acetylcholine receptors with as many as three kinds of subunits and can segregate subunits among receptor subtypes. Neuron 10:451–464.
Wada E, Wada K, Boulter J, Deneris E, Heinemann S, Patrick J, Swanson LW (1989) Distribution of α2, α3, α4, and β2 neuronal nicotinic receptor subunit mRNAs in the central nervous system: a hybridization histochemical study in the rat. J Comp Neurol 284:314–335.
Wada E, McKinnon D, Heinemann S, Patrick J, Swanson LW (1990) The distribution of mRNA encoded by a new member of the neuronal nicotinic acetylcholine receptor gene family (α5) in the rat central nervous system. Brain Res 526:45–53.
Wamsley JK, Gehlert DR, Roeske WR, Yamamura HI (1984) Muscarinic antagonist binding site heterogeneity as evidenced by autoradiography after direct labeling with [^{3}H]-QNB and [^{3}H]-pirenzepine. Life Sci 34:1395–1402.
Wang F, Gerzanich V, Wells GB, Anand R, Peng X, Keyser K, Lindstrom J (1996) Assembly of human neuronal nicotinic receptor α5 subunits with α3, β2, and β4 subunits. J Biol Chem 271:17656–17665.
Zoli M, Le Novère N, Hill Jr JA, Changeux JP (1995) Developmental regulation of nicotinic receptor subunit mRNAs in the rat central and peripheral nervous systems. J Neurosci 15:1912–1939.